

# Lepton Flavor Universality at Belle and Belle II

Seema Choudhury<sup>1,\*</sup> on behalf of Belle and Belle II collaborations

<sup>1</sup>Iowa State University and High Energy Accelerator Research Organization

**Abstract.** We report the test of lepton flavor universality at Belle and Belle II experiments considering  $b \rightarrow c$  and  $b \rightarrow s$  transitions. We use  $711 \text{ fb}^{-1}$  and  $189 \text{ fb}^{-1}$  of data collected at  $\Upsilon(4S)$  resonance from electron-positron collisions for Belle and Belle II, respectively. For the  $b \rightarrow c$  transition, we present the measurement of lepton-flavor-universality in  $B^0 \rightarrow D^{*\ell^+}\nu_\ell$  decay, exclusive measurement of  $\mathcal{R}(D)$  &  $\mathcal{R}(D^*)$  in Belle data, and inclusive  $R(X_{e/\mu})$  in Belle II. For the  $b \rightarrow s$  transitions, we provide measurements of  $R_K$  and  $R_{K^*}$  using Belle data, measurement of the branching fraction for the decay  $B \rightarrow K^*\ell\ell$ , and test of lepton-flavor-universality in  $B \rightarrow J/\psi K$  using Belle II data. Additionally, we report the lepton-flavor-universality in  $\Omega_c^0 \rightarrow \Omega^-\ell^+\nu_\ell$  decay using  $922 \text{ fb}^{-1}$  of data collected by the Belle detector.

## 1 Belle and Belle II detectors

KEKB was an asymmetric energy  $e^+$  (3.5 GeV) -  $e^-$  (8 GeV) collider with center-of-mass (CM) energy at the  $B\bar{B}$  threshold corresponds to 10.58 GeV. Belle [1] detector was situated at the interaction point of the  $e^+e^-$ . It has collected 711, 89.5, and  $121.1 \text{ fb}^{-1}$  data at the CM energies 10.58, 10.52, and 10.86 GeV, respectively from 1999 to 2010. The detector consisted of many sub-detectors to identify different charged and neutral particles. Belle II [2] is the successor of the Belle experiment with  $e^+$  and  $e^-$  energies of 4 GeV and 7 GeV respectively, successfully collecting data from 2019. It aims at collecting  $50 \text{ ab}^{-1}$  of data by 2035 and plans to deliver collision at a peak luminosity of  $6.5 \times 10^{35} \text{ cm}^{-2}\text{s}^{-1}$  [2] (30 times that of KEKB). The increase in peak luminosity is contributed by the reduction in the beam size by 20 times and 1.5 times increase in beam current. The Belle II detector is also upgraded to cope-up with the beam background which increases in proportion to the luminosity. Belle II has collected  $\sim 424 \text{ fb}^{-1}$  data sample to date, having 364, 42, and  $19 \text{ fb}^{-1}$  at 10.58, 10.52, and 10.75 GeV, respectively. Belle II has a world record instantaneous luminosity of  $4.71 \times 10^{34} \text{ cm}^{-2}\text{s}^{-1}$  on 22<sup>nd</sup> June 2022.

## 2 LFU in $b \rightarrow c$ transition

The  $B$  decays with  $b \rightarrow c$  tree-level transition are an important probe to test the lepton-flavor-universality (LFU). The ratio of exclusive decays with  $\tau$  lepton can be used to test the standard model (SM) by measuring  $\mathcal{R}(D^{(*)}) = \frac{\mathcal{B}(B \rightarrow D^{(*)}\tau\nu)}{\mathcal{B}(B \rightarrow D^{(*)}\ell\nu)}$ , where  $\ell = e, \mu$ . The combined result from Belle [3–5], BaBar [6], and LHCb [7, 8] has a tension of  $3.1\sigma$  with

\*e-mail: [seema.choudhury@kek.jp](mailto:seema.choudhury@kek.jp)

SM [9]. The LFU test can also be performed by measuring  $R(X) = \frac{\mathcal{B}(B \rightarrow X\tau\nu)}{\mathcal{B}(B \rightarrow X\ell\nu)}$ , which is the complimentary measurement to  $\mathcal{R}(D^{(*)})$  via inclusive reconstruction. The  $R(X)$  measurement is more challenging due to the background from a less constrained  $X$  system. The LFU can be tested using light leptons by measuring  $R(X_{e/\mu})$ .

## 2.1 Measurement of LFU in $B^0 \rightarrow D^{*-}\ell\nu_\ell$ at Belle

Belle [10] has performed the LFU measurement in exclusive semileptonic  $B$  decay using  $B^0 \rightarrow D^{*-}(\bar{D}^0(K^+\pi^-\pi^-)\ell\nu_\ell)$  decay with a data sample of  $711 \text{ fb}^{-1}$ . The analysis is done using an untagged approach, leading to high efficiency with a sizable background. The background from fake  $D^*$  is suppressed by constraining  $D^*$  momentum in the CM frame to be  $< 2.45 \text{ GeV}/c$ . The signal yield is extracted with a 3-dimensional binned maximum likelihood (ML) fit to  $\cos\theta_{B,D^*\ell}$  ( $\frac{2E_B^*E_{D^*\ell} - m_B^2 - m_{D^*\ell}^2}{2|p_B^*||p_{D^*\ell}|}$ ),  $\Delta M = M(D^* - D^0)$ , and lepton momentum ( $p_\ell$ ). The results are shown in Fig. 1. The ratio of the branching fractions of modes with electrons

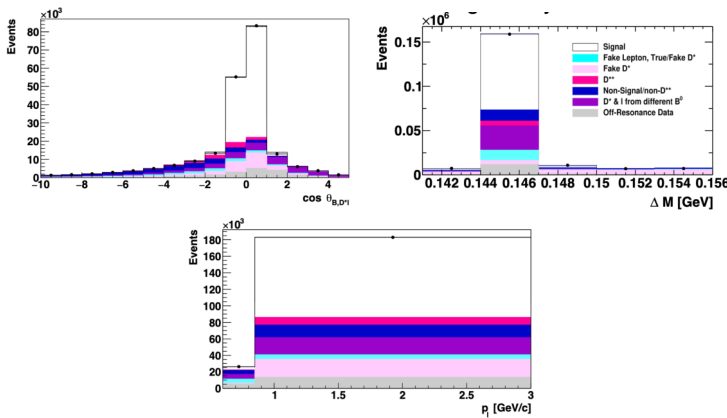


**Figure 1.** Fits to the  $\cos\theta_B$  (top-left),  $\Delta M$  (top-right), and  $p_\ell$  (bottom) in the  $\mu$  mode. The points represent the data.

and muons provides a test of the LFU, *i.e.*,  $\frac{\mathcal{B}(B^0 \rightarrow D^{*-}e^+\nu_e)}{\mathcal{B}(B^0 \rightarrow D^{*-}\mu^+\nu_\mu)} = 1.01 \pm 0.01(\text{stat}) \pm 0.03(\text{sys})$ .

The result is consistent with unity within the uncertainty.

## 2.2 Measurement of $\mathcal{R}(D)$ & $\mathcal{R}(D^*)$ at Belle

Belle [5] has measured simultaneously  $\mathcal{R}(D)$  and  $\mathcal{R}(D^*)$  using the semileptonic tagging method. Here, the tag-side  $B$  is reconstructed via  $B^{0/\pm} \rightarrow D^{(*)}\ell^-\nu$  decay and signal side  $B$  from  $B^{0/\pm} \rightarrow D^{(*)}\tau^-(\ell^-\bar{\nu})\nu$ , the normalization channel is  $B^{0/\pm} \rightarrow D^{(*)}\ell^-\nu$ . The tagging method ensures good signal purity at the cost of lower signal reconstruction efficiency. The signal is extracted with 2-dimensional binned ML fit to the energies of neutral clusters detected in the ECL that are not associated with any reconstructed particles ( $E_{ECL}$ ) and the background suppression classifier output ( $O_{cls}$ ). The fit results are shown in Fig. 2. The measured value of  $\mathcal{R}(D) = 0.307 \pm 0.037(\text{stat}) \pm 0.016(\text{sys})$  and  $\mathcal{R}(D^*) = 0.283 \pm 0.018(\text{stat}) \pm 0.014(\text{sys})$  have deviations of  $0.2\sigma$  and  $1.1\sigma$ , respectively. The combined result of  $\mathcal{R}(D)$  &  $\mathcal{R}(D^*)$  has a deviation of  $0.8\sigma$ .

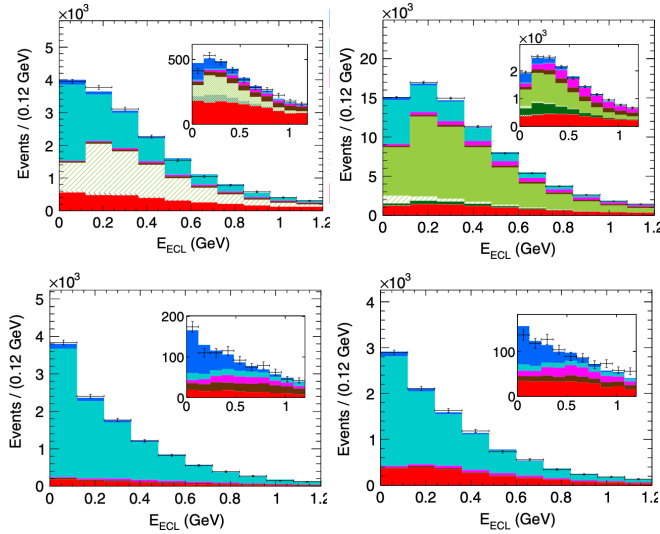


**Figure 2.**  $E_{ECL}$  fit projection and data points with statistical uncertainties in the  $D^+ \ell^-$  (top-left),  $D^0 \ell^-$  (top-right),  $D^{*+} \ell^-$  (bottom-left), and  $D^{*0} \ell^-$  (bottom-right) samples. The signal enhanced region is shown in the inset.

### 2.3 Measurement of $R(X_{e/\mu})$ at Belle II

Belle II [11] has checked the LFU by inclusive measurement of  $R(X_{e/\mu})$  using  $189 \text{ fb}^{-1}$  of data sample with hadronic- $B$  tagging approach. In this measurement, the signal side  $B$  flavor and kinematics is constrained by tagging the other  $B$  in its fully hadronic decays, which leads to good signal purity at a cost of lower signal reconstruction efficiency. The  $X$  system on the signal side contains a large variety of different charged and neutral final-state particles. As we reconstruct only the lepton in the signal side, the lepton momentum in the  $B$  signal rest frame,  $p_\ell^*$ , is used to extract the signal yield. We required the lepton to have a high probability to be an electron or muon and  $p_\ell^* > 1.3 \text{ GeV}/c$  to suppress backgrounds from hadrons faking as leptons and secondary leptons from  $b \rightarrow c \rightarrow (\ell, s)$  cascades and  $B \rightarrow X\tau\nu$ . The signal yields for  $B \rightarrow X e \nu$  and  $B \rightarrow X \mu \nu$  channels are extracted simultaneously in 10 bins of  $p_\ell^*$ , with one-dimensional binned ML fit. The fit results are shown in Fig. 3. There are  $48034 \pm 286$ ,  $58569 \pm 429$  signal events for  $B \rightarrow X e \nu$  and  $B \rightarrow X \mu \nu$  channels, respectively. The  $R(X_{e/\mu})$  measured to be  $1.033 \pm 0.010(\text{stat}) \pm 0.020(\text{sys})$ , for  $p_\ell^* > 1.3 \text{ GeV}/c$ . This is the first inclusive test of  $(e, \mu)$  lepton flavor universality in semileptonic  $B \rightarrow X \ell \nu$  decays. The measurement is in agreement with unity within  $1.5\sigma$ , with a world-leading precision of 2.2%. This measurement paved the path for  $R(X) = R(X_{\tau/\ell})$  measurement.

### 3 LFU in $b \rightarrow s$ transition

$b \rightarrow s$  is propagated through loop-level transition and is an important probe to test the LFU by measuring  $R_K$  and  $R_{K^*}$  for  $B \rightarrow K \ell \ell$  and  $B \rightarrow K^* \ell \ell$  decays, *i.e.*,  $R_{K^{(*)}} = \frac{\mathcal{B}(B \rightarrow K^{(*)} \mu \mu)}{\mathcal{B}(B \rightarrow K^{(*)} e e)}$ . According to SM this ratio should be 1 [12], as the coupling of leptons to gauge boson is independent of flavor. LHCb [13] has reported a deviation of  $3.1\sigma$  in  $R_{K^*}$  measurement for  $q^2 \in [1.1 - 6.0] \text{ GeV}^2/c^4$  bin using  $9 \text{ fb}^{-1}$  data sample,  $q^2$  is invariant mass square of lepton

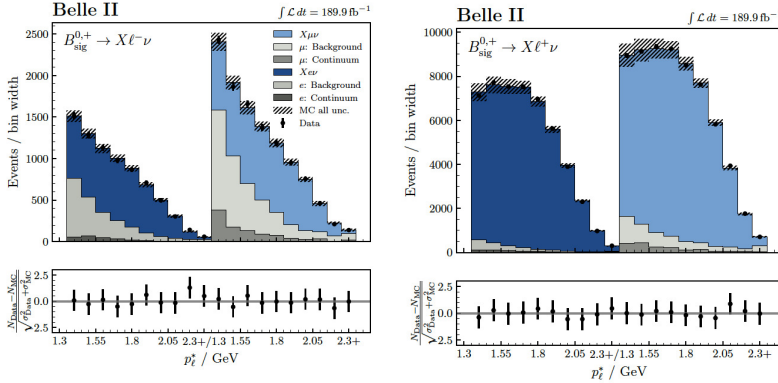


**Figure 3.** Distributions of Lepton momentum in the  $B_{\text{sig}}$  frame ( $p_\ell^*$ ) in the correct sign (left) and wrong sign (right). The electron and muon templates are fitted simultaneously in  $10p_\ell^*$  bins with a width of 100 MeV each covering a  $p_\ell^*$  range from 1.3 GeV to 2.3 GeV.

pair. Similarly,  $R_{K^{++}}$  and  $R_{K_S^0}$  measurements from LHCb [14] have  $1.4\sigma$  and  $1.5\sigma$  deviations from SM, calculated in  $3 \text{ fb}^{-1}$  data sample.

### 3.1 $R_{K^*}$ measurement at Belle

Belle [15] has measured  $R_{K^*}$  using a full data sample of  $711 \text{ fb}^{-1}$ . The decay modes reconstructed are  $B^+ \rightarrow K^{*+}(K^+\pi^0, K_S^0\pi^+)\ell\ell$  and  $B^0 \rightarrow K^{*0}(K^+\pi^-, K_S^0\pi^0)\ell\ell$ . The kinematic variables which distinguish the signal from the background are beam-energy-constrained mass,  $M_{\text{bc}} = \sqrt{E_{\text{beam}}^2/c^4 - |p_B|^2/c^2}$  and energy difference,  $\Delta E = E_B - E_{\text{beam}}$ . Here,  $p_B$  and  $E_B$  are the momentum and energy of the  $B$  candidate, and  $E_{\text{beam}}$  is the beam energy. The background coming from the continuum and  $B\bar{B}$  are suppressed using Neural Network (NN). The signal yield is obtained by performing a 1-dimensional unbinned extended ML fit in  $M_{\text{bc}}$ , shown in Fig. 4. From the fit, the signal yields are  $103^{+13.4}_{-12.7}$  and  $139.9^{+16.0}_{-15.4}$  for electron and muon channels, respectively. From the fitted signal yield and signal MC efficiency, the  $R_{K^*}$  is calculated for charged  $B$ , neutral  $B$ , and the combined result from charged and neutral  $B$ , as shown in Fig. 5. The results for different bins are consistent with SM expectations within the uncertainty.

### 3.2 $R_K$ measurement at Belle

$R_K$  tests LFU in  $B \rightarrow K\ell\ell$  decays. The analysis is performed in  $711 \text{ fb}^{-1}$  data sample of Belle [16]. The decay modes reconstructed are  $B^+ \rightarrow K^+\ell\ell$  and  $B^0 \rightarrow K_S^0\ell\ell$ . The background from continuum and  $B\bar{B}$  are suppressed using a NN which uses several event shapes, vertex quality, and kinematic variables. The signal yield is extracted by 3-dimensional unbinned extended ML fit in  $M_{\text{bc}}$ ,  $\Delta E$ , and the translated NN output ( $O'$ ). The fit results are shown in Fig. 6. There are  $137 \pm 14$ ,  $138 \pm 15$ ,  $27.3^{+6.6}_{-5.8}$ , and  $21.8^{+7.0}_{-6.1}$  signal events for  $B^+ \rightarrow K^+\mu\mu$ ,  $B^+ \rightarrow K^+ee$ ,  $B^0 \rightarrow K_S^0\mu\mu$ , and  $B^0 \rightarrow K_S^0ee$ , respectively. The  $R_{K^+}$ ,  $R_{K^0}$ , and  $R_K$  are measured in different  $q^2$  bins, as shown in Fig. 7. The results are in agreement with SM expectations within the uncertainty. In addition to this, we have the most precise measurement for  $R_K$  in the  $J/\psi$  region and is consistent with the unity, *i.e.*,  $R_{K^+}(J/\psi) = 0.994 \pm 0.011(\text{stat}) \pm 0.010(\text{sys})$  and  $R_{K^0}(J/\psi) = 0.993 \pm 0.015(\text{stat}) \pm 0.010(\text{sys})$ .

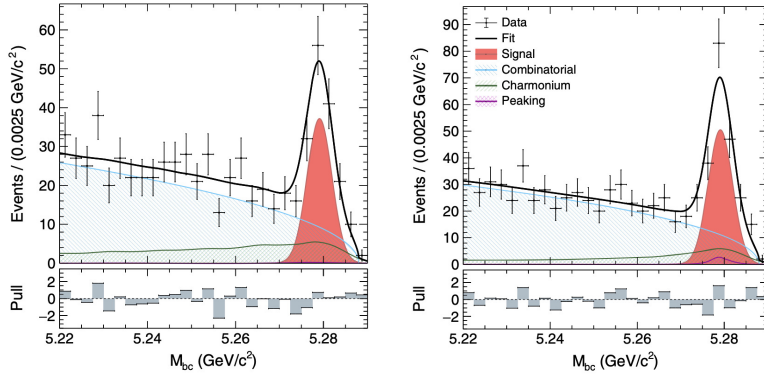


**Figure 4.** Fit result of  $B \rightarrow K^* \ell \ell$  in terms of  $M_{bc}$  for the electron (left) and muon (right) modes with  $q^2 > 0.045 \text{ GeV}^2/c^4$ . Combinatorial (dashed blue), signal (red filled), charmonium (dashed green), peaking (purple dotted), and total (solid) fit distributions are superimposed on data (points with error bars).

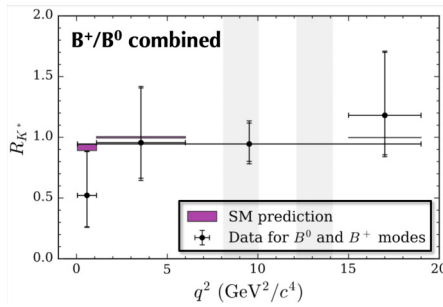


**Figure 5.** Result for  $R_{K^*}$  compared to SM predictions in bins of  $q^2 \in [0.045, 1.1], [1.1, 6], [15, 19],$  and  $[0.045, 19] \text{ GeV}^2/c^4$ . The shaded bands indicate the charmonium vetoes.

### 3.3 Measurement of $\mathcal{B}(B \rightarrow K^* \ell \ell)$ at Belle II

Belle II [17] has measured  $\mathcal{B}(B \rightarrow K^* \ell \ell)$  using  $190 \text{ fb}^{-1}$  of data. For this analysis, the decay modes reconstructed are  $B^0 \rightarrow K^{*0}(K^+ \pi^-) \ell \ell$  and  $B^+ \rightarrow K^{*+}(K^+ \pi^0, K_S^0 \pi^+) \ell \ell$ . The signal yield is extracted by 2-dimensional un-binned extended ML fit in  $M_{bc}$  and  $\Delta E$  for the events which pass tight requirement on the boosted decision tree, used to fight the background from continuum and  $B\bar{B}$ . The fit results are shown in Fig. 8. The branching fractions are measured for the entire range of the dilepton mass, excluding the mass region to suppress the  $B \rightarrow K^* \gamma (\rightarrow e^+ e^-)$  background and the regions compatible with decays of charmonium resonances to be;  $\mathcal{B}(B \rightarrow K^*(892) \mu^+ \mu^-) = (1.19 \pm 0.31(\text{stat})_{-0.07}^{+0.08}(\text{sys})) \times 10^{-6}$ ,  $\mathcal{B}(B \rightarrow K^*(892) e^+ e^-) = (1.42 \pm 0.48(\text{stat}) \pm 0.09(\text{sys})) \times 10^{-6}$ , and  $\mathcal{B}(B \rightarrow K^*(892) \ell^+ \ell^-) = (1.25 \pm 0.30(\text{stat})_{-0.07}^{+0.08}(\text{sys})) \times 10^{-6}$ . The results are compatible with the world averages within the uncertainties. This is a preliminary step towards the LFU test using larger data sample of Belle II.

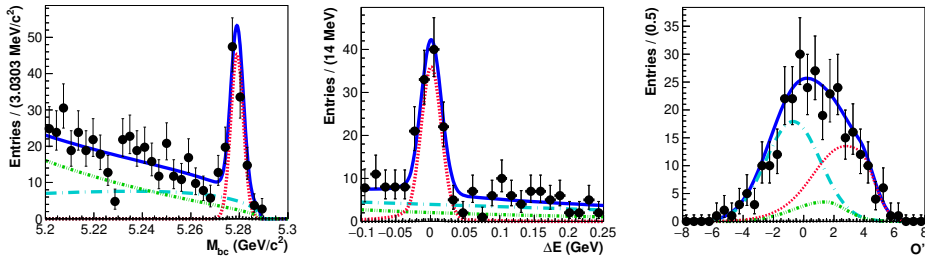


**Figure 6.** Signal-enhanced  $M_{bc}$  (left),  $\Delta E$  (middle), and  $O'$  (right) projections for  $B^+ \rightarrow K^+ \mu\mu$  decay. Point with error bars are the data, blue solid curves are the fitted result, red dashed curves denote the signal component, cyan long dashed, green dash-dotted, and black dashed curves represent continuum,  $B\bar{B}$  background, and  $B \rightarrow$  charmless decays, respectively.

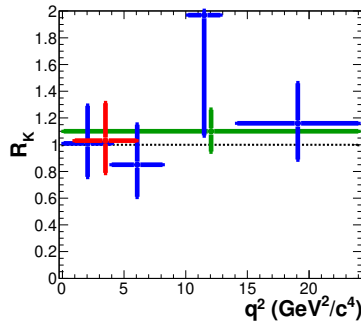


**Figure 7.**  $R_K$  in bins of  $q^2$  for  $B \rightarrow K\ell\ell$ . The red marker represents the bin of  $1.0 < q^2 < 6.0$   $\text{GeV}^2/c^4$ , and the blue marker are for  $0.1 < q^2 < 4.0$ ,  $4.00 < q^2 < 8.12$ ,  $10.2 < q^2 < 12.8$ , and  $q^2 > 14.18$   $\text{GeV}^2/c^4$  bins. The green marker denotes the whole  $q^2$  region excluding the charmonium resonances.

### 3.4 Measurement of $R_K(J/\psi)$ at Belle II

Belle II [18] has tested LFU in  $B \rightarrow J/\psi K$  using  $190 \text{ fb}^{-1}$  data sample. The decay modes reconstructed are  $B^+ \rightarrow J/\psi(\ell\ell)K^+$  and  $B^0 \rightarrow J/\psi(\ell\ell)K^0$ . The signal yield is obtained by 2-dimensional un-binned extended ML fit in  $M_{bc}$  and  $\Delta E$ . The fit results are shown in Fig. 9. The signal has a purity of 90–95%. The LFU ratio measured from charged and neutral  $B$  are  $R_{K^+}(J/\psi) = 1.009 \pm 0.022(\text{stat}) \pm 0.008(\text{sys})$  and  $R_{K^0}(J/\psi) = 1.042 \pm 0.042(\text{stat}) \pm 0.008(\text{sys})$ , respectively. These results are statistically dominated and in agreement with PDG [19].

## 4 Measurement of $R(\Omega)$ at Belle

LFU in  $\Omega_c^0$  is probed for the first time with  $\Omega_c^0 \rightarrow \Omega^- \ell^+ \nu_\ell$  decay using Belle [20] data sample of  $922 \text{ fb}^{-1}$ . The data of 89.5, 711, and  $121.1 \text{ fb}^{-1}$  are collected at the CM energies of 10.52, 10.58, and 10.86 GeV, respectively. These decays are reconstructed in the process  $e^+e^- \rightarrow c\bar{c} \rightarrow \Omega_c^0 + \text{anything}$ . The signal yield is extracted by binned ML fit to the invariant mass ( $M_{\Omega\ell}$ ) spectra. The fit results are shown in Fig. 10. The signal yields for  $\Omega_c^0 \rightarrow \Omega^- \pi^+$ ,  $\Omega_c^0 \rightarrow \Omega^- e^+ \nu_e$ , and  $\Omega_c^0 \rightarrow \Omega^- \mu^+ \nu_\mu$  are  $865.3 \pm 35.3$ ,  $707.6 \pm 37.7$ , and  $367.9 \pm 31.4$  events,

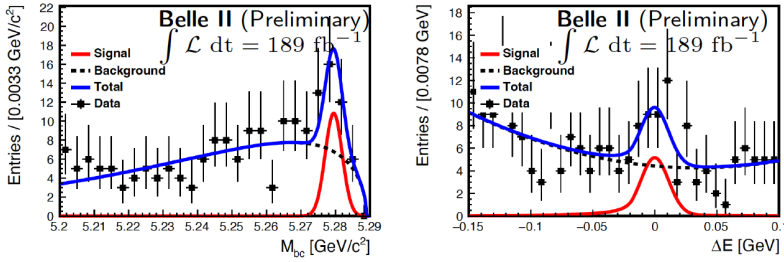


**Figure 8.**  $M_{bc}$  (left) and  $\Delta E$  (right) projection for  $B \rightarrow K^* \ell \ell$  decay. Points with error bars are superimposed on the blue (solid) curve showing total fit result, while red (solid) and black (dotted) lines represent the signal and background components.

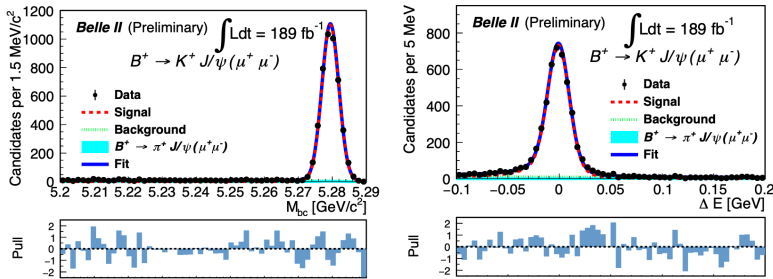


**Figure 9.**  $M_{bc}$  (left) and  $\Delta E$  (right) distributions with the fit result superimposed. Black dots with error bars denote the data, blue curve denote the total fit, dashed red curves are the signal component, dotted green curves are the background component, and filled cyan regions are the  $B^* \rightarrow J/\psi \pi^+$  component.

respectively. The significance of the  $\Omega_c^0 \rightarrow \Omega^- \ell^+ \nu_\ell$  are both larger than  $10\sigma$ , and  $\Omega_c^0 \rightarrow \Omega^- \mu^+ \nu_\ell$  decay is seen for the first time in Belle, where  $\Omega_c^0 \rightarrow \Omega^- \pi^+$  decay is used as a normalization channel. The semileptonic decay branching fraction ratio is calculated to be;  $R(\Omega) = \frac{\mathcal{B}(\Omega_c^0 \rightarrow \Omega^- e^+ \nu_e)}{\mathcal{B}(\Omega_c^0 \rightarrow \Omega^- \mu^+ \nu_\mu)} = 1.02 \pm 0.10(\text{stat}) \pm 0.02(\text{sys})$ . The  $R(\Omega)$  agrees with the expected LFU value  $1.03 \pm 0.06$  [21] within the uncertainty.

## 5 LFU prospects at Belle II

The  $R(X)$  measurement or in general inclusive processes are unique to Belle II. The estimated precision on  $R(X)$  for  $189 \text{ fb}^{-1}$  of data sample is  $\sim 17\%$ . The uncertainty (statistical + systematic) projections for  $\mathcal{R}(D)$ ,  $\mathcal{R}(D^*)$ , and  $R(X)$  are shown in Fig. 11 [22]. A few  $\text{ab}^{-1}$  of data from Belle II will be sufficient to track the anomaly on  $\mathcal{R}(D) - \mathcal{R}(D^*)$  to be statistical or systematic origin. With the full data sample of Belle II, the total uncertainty for  $\mathcal{R}(D) - \mathcal{R}(D^*)$  will be 2 – 3% for different tagging approaches (semileptonic or hadronic).  $R(X)$  will also be of similar precision. Similarly, for  $b \rightarrow s$  transition, the  $R_{K^*}$  projections for  $1 \text{ ab}^{-1}$ ,  $5 \text{ ab}^{-1}$ , and  $50 \text{ ab}^{-1}$  are shown in Fig. 11. The  $R_{K^+}$  and  $R_{K^*}$  statistical sensitivity will be  $< 2\%$  for the entire  $q^2$  region and  $\sim 3\%$  for  $q^2 \in [1-6] \text{ GeV}^2/c^4$ , with full data sample of  $50 \text{ ab}^{-1}$ . Contrary to LHCb, Belle II can check these observables both for low and high  $q^2$  bins. Belle II will

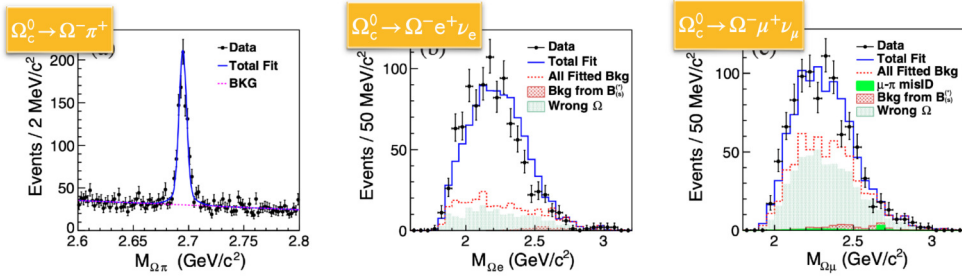


**Figure 10.** Fit to the  $M_{\Omega\pi}$  (left),  $M_{\Omega e}$  (middle),  $M_{\Omega\mu}$  (right) distributions. The dots with error bars represent the data, the solid lines are the best fits, and the dashed lines are the fitted total background. The blank areas between the red dashed lines and shaded histograms are from backgrounds with mis-selected  $\ell^+$ . The  $\mu - \pi$  misID in  $M_{\Omega\mu}$  plot is the background from  $\Omega_c^0 \rightarrow \Omega^- \pi^+ + \text{hadrons}$  decays.

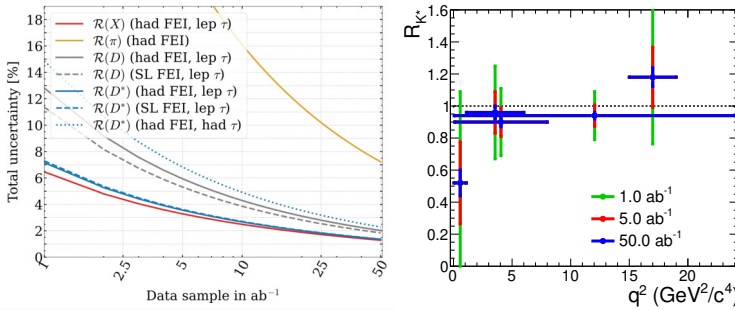


**Figure 11.** LFU prospects of Belle II for  $b \rightarrow c$  (left) and  $b \rightarrow s$  (right) transitions.

provide an independent measurement to confirm the tension observed in  $R_K - R_{K^*}$  with few  $\text{ab}^{-1}$  of data sample.

## 6 Summary

The flavor physics in  $e^+e^-$  collisions offers an extremely rich physics program with many opportunities to probe physics beyond the SM. At Belle II, we can access charged and neutral  $B$  with equal efficiency and also have equal sensitivity for electron and muon channels. Belle II can access inclusive decay modes in addition to exclusive decays, and analysis can be performed in tagged or un-tagged approaches. Belle II has collected  $\sim 424 \text{ fb}^{-1}$  of data which is comparable to the size of the BaBar data sample and can be combined with the Belle data sample to increase statistics. So far, Belle or Belle II have not observed any sign of LFU violation and a higher data sample will shed light on LFU anomalies. Some results show the potential of Belle II, and only a part of them are covered here. We will have more results from Belle II in near future.

## References

[1] A. Abashian *et al.* (Belle Collaboration), Nucl. Instrum. Methods Phys. Res., Sec. A 479, 117 (2002); also, see the detector section in J. Brodzicka *et al.*, Prog. Theor. Exp. Phys.



**2012**, 04D001 (2012).

- [2] T. Abe *et al.* (Belle II Collaboration), arXiv:1011.0352.
- [3] M. Huschle *et al.* (Belle Collaboration), Phys. Rev. D **92**, 072014 (2015).
- [4] S. Hirose *et al.* (Belle Collaboration), Phys. Rev. Lett. **118**, 211801 (2017).
- [5] G. Caria *et al.* (Belle Collaboration), Phys. Rev. Lett. **124** 161803 (2020).
- [6] J. P. Lees *et al.* (BaBar Collaboration), Phys. Rev. D **88**, 072012 (2013).
- [7] R. Aaij *et al.* (LHCb Collaboration), Phys. Rev. Lett. **115**, 111803 (2015).
- [8] R. Aaij *et al.* (LHCb Collaboration), Phys. Rev. D **97**, 072013 (2018).
- [9] Y. Amhis *et al.* (HFLAV Collaboration), arXiv:2206.07501.
- [10] E. Waheed *et al.* (Belle Collaboration), Phys. Rev. D **100**, 052007 (2019).
- [11] H. Junkerkalefeld *et al.* (Belle II Collaboration), ICHEP 2022.
- [12] M. Bordone, G. Isidori, and A. Pattori, Eur. Phys. J. C **76**, 440 (2016).
- [13] R. Aaij *et al.* (LHCb Collaboration), Nature Physics **18**, 277 (2022).
- [14] A. Aaij *et al.* (LHCb Collaboration), Phys. Rev. Lett. **128**, 191802 (2022).
- [15] S. Wehle *et al.* (Belle Collaboration), Phys. Rev. Lett. **126**, 161801 (2021).
- [16] S. Choudhury *et al.* (Belle Collaboration), J. High Energy Phys. **03**, 105 (2021)
- [17] F. Abudinén *et al.* (Belle II Collaboration), arXiv:2206.05946.
- [18] F. Abudinén *et al.* (Belle II Collaboration), arXiv:2207.11275.
- [19] P.A. Zyla *et al.* (Particle Data Group), Prog. Theor. Exp. Phys. **2020**, 083C01 (2020).
- [20] Y. B. Li *et al.* (Belle Collaboration), Phys. Rev. D **105**, L091101 (2022).
- [21] F. Huang, Q. A. Zhang, arXiv:2108.06110.
- [22] Snowmass 2021, arXiv: 2207.06307.